

# Neuronal Adaptation Caused by Sequential Visual Stimulation in the Frontal Eye Field

J. Patrick Mayo and Marc A. Sommer

*J Neurophysiol* 100:1923-1935, 2008. First published 6 August 2008;

doi: 10.1152/jn.90549.2008

## You might find this additional info useful...

---

This article cites 67 articles, 31 of which you can access for free at:

<http://jn.physiology.org/content/100/4/1923.full#ref-list-1>

This article has been cited by 3 other HighWire-hosted articles:

<http://jn.physiology.org/content/100/4/1923#cited-by>

Updated information and services including high resolution figures, can be found at:

<http://jn.physiology.org/content/100/4/1923.full>

Additional material and information about *Journal of Neurophysiology* can be found at:

<http://www.the-aps.org/publications/jn>

---

This information is current as of August 8, 2012.

# Neuronal Adaptation Caused by Sequential Visual Stimulation in the Frontal Eye Field

J. Patrick Mayo and Marc A. Sommer

*Department of Neuroscience, Center for Neuroscience at the University of Pittsburgh, Center for the Neural Basis of Cognition, University of Pittsburgh, Pittsburgh, Pennsylvania*

Submitted 10 May 2008; accepted in final form 29 July 2008

**Mayo JP, Sommer MA.** Neuronal adaptation caused by sequential visual stimulation in the frontal eye field. *J Neurophysiol* 100: 1923–1935, 2008. First published April 6, 2008; doi:10.1152/jn.90549.2008. Images on the retina can change drastically in only a few milliseconds. A robust description of visual temporal processing is therefore necessary to understand visual analysis in the real world. To this end, we studied subsecond visual changes and asked how prefrontal neurons in monkeys respond to stimuli presented in quick succession. We recorded the visual responses of single neurons in the frontal eye field (FEF), a prefrontal area polysynaptically removed from the retina that is involved with higher level cognition. For comparison, we also recorded from small groups of neurons in the superficial superior colliculus (supSC), an area that receives direct retinal input. Two sequential flashes of light at varying interstimulus intervals were presented in a neuron's receptive field. We found pervasive neuronal adaptation in FEF and supSC. Visual responses to the second stimulus were diminished for up to half a second after the first stimulus presentation. Adaptation required a similar amount of time to return to full responsiveness in both structures, but there was significantly more neuronal adaptation overall in FEF. Adaptation was not affected by saccades, although visual responses to single stimuli were transiently suppressed postsaccadically. Our FEF and supSC results systematically document subsecond visual adaptation in prefrontal cortex and show that this adaptation is comparable to, but stronger than, adaptation found earlier in the visual system.

## INTRODUCTION

The frontal eye field (FEF) in prefrontal cortex has been implicated in visual analysis, cognitive processing, and saccade generation (Bruce and Goldberg 1985; Bruce et al. 1985; Schall 2002). These functions require precise spatial and temporal organization. Whereas a long history of research has studied the spatial properties of FEF neurons (Bruce and Goldberg 1985; Mohler et al. 1973; Umeno and Goldberg 1997, 2001), much less is known about the temporal properties of FEF visual responses. In other visual areas, presenting two visual stimuli in quick succession has a profound effect on neuronal activity; the response to the second stimulus is severely diminished. We term this phenomenon “neuronal adaptation.” Such adaptation has been found in many parts of the brain (IT: Baylis and Rolls 1987; Brown et al. 1987; V1: Judge et al. 1980a; V4: Motter 2006; LGN: Schiller 1968; for review, see Kohn 2007), but has never been characterized in FEF.

Understanding the temporal aspects of FEF neuronal activity is critical for three reasons. First, to provide insight into the neuronal basis of cognition, experiments on cognitive process-

ing in FEF may benefit from using two or more visual stimuli flashed in quick succession (Thompson and Schall 1999). Neuronal adaptation could influence the results of such studies. The extent to which FEF neurons are susceptible to adaptation, however, is unknown.

Second, understanding subsecond temporal processing is important for determining how the visual system processes natural visual scenes. Many real world changes (e.g., visibility of prey or the actions of a predator) occur at subsecond time scales that are outside the temporal boundaries of most previous electrophysiological studies, especially those performed in frontal cortex. Thus it is crucial to establish the fundamental temporal characteristics of FEF visual activity at a fast, ecologically relevant time scale.

Last, the study of visual timing is critical for understanding how movements influence perception. It has been shown that temporal judgments about visual stimuli change around the time of a saccade. Specifically, perceived durations shorten presaccadically and lengthen postsaccadically (Georg and Lappe 2007; Matin et al. 1972; Morrone et al. 2005; Yarrow et al. 2001). As an interface between vision and eye movements (Schall 2002), FEF seems well positioned to play a central role in such temporal effects.

The first step in understanding temporal influences on visual processing in FEF is to study neuronal adaptation caused by two sequentially presented stimuli. We asked whether adaptation occurs for FEF neurons, and if so, how it is affected by interstimulus interval (ISI) and saccade generation. As a point of comparison, and to verify our methods, we additionally studied adaptation in neurons in the retinal-recipient superficial layers of the superior colliculus (supSC), an important visuosaccadic structure located in the midbrain. Neuronal adaptation in SC has been well characterized in previous work (Dorris et al. 2002; Fecteau and Munoz 2005; Robinson and Kertzman 1995; Wurtz et al. 1980). We predicted that the direct retinal input to supSC, compared with the absence of such input to FEF, would lead to relatively reduced levels of neuronal adaptation in the subcortical structure.

We found that neuronal adaptation in both FEF and supSC is strong for ISIs <100 ms, weaker for relatively longer ISIs, and absent for ISIs >400 ms. Neurons in FEF showed significantly more adaptation than neurons in supSC. For both FEF and supSC, we found no difference in adaptation immediately after a saccade, compared with during steady fixation, despite clear suppression of the visual response itself postsaccadically.

Address for reprint requests and other correspondence: J. P. Mayo, Dept. of Neuroscience, A210 Langley Hall, Univ. of Pittsburgh, Pittsburgh, PA 15260 (E-mail: jpm49@pitt.edu).

The costs of publication of this article were defrayed in part by the payment of page charges. The article must therefore be hereby marked “advertisement” in accordance with 18 U.S.C. Section 1734 solely to indicate this fact.

Our results show differences in duration-dependent visual responses at contrasting levels of visual processing. Furthermore, they provide a foundation for carrying out future studies in FEF using visual stimuli presented at real-world time scales.

## METHODS

Two probes were presented consecutively (i.e., temporally non-overlapping) in the receptive field (RF) of a neuron while the animal fixated. The probes were identical but appeared at slightly different locations near the RF center to minimize afterimages and lower-level adaptation effects (Marlin et al. 1991; Movshon and Lennie 1979). We varied the amount of time between the two probes and included single probe control conditions to help quantify the temporal dynamics of neuronal activity in response to repeated visual stimulation. We developed the metric “penetrance” to quantify the extent to which a visual response was evoked by the second visual stimulus of a successive pair of stimuli.

### Animals and surgery

Four rhesus monkeys (*Maccaca mulatta*; monkeys C, K, M, and N) were anesthetized and surgically prepared for neuronal recordings and eye position measurements. Using aseptic procedures, titanium screws and an acrylic implant were affixed to the skull. Recording chambers and a head-restraint socket (Crist Instruments, Hagerstown, MD) were embedded in the implant. Chambers were positioned over FEF (monkeys C, K, and N) and supSC (monkeys K and M) using stereotaxic coordinates (FEF: A23 and L20; SC: angled 40° posterior from vertical, centered mediolaterally on the midline, and aimed at a location 1 mm posterior and 15 mm above stereotaxic zero). In the same surgery, we implanted scleral search coils (Judge et al. 1980b). Animals recovered for  $\geq 1$ –2 wk before training resumed. All experimental procedures were approved by and conducted under the auspices of the University of Pittsburgh Institutional Animal Care and Use Committee and were in compliance with the guidelines set forth in the United States Public Health Service Guide for the Care and Use of Laboratory Animals.

### Behavior

We trained monkeys to perform a simple visually guided saccade task to targets while other visual stimuli (“probes”) were flashed in the RF (Fig. 1). The probes were irrelevant to the task demands for reward. A head-restrained monkey viewed visual stimuli that were projected onto a tangent screen. Every trial began with the presentation of a fixation spot (Fig. 1, cross) in the center of the screen. After foveating the spot, the monkey was required to maintain fixation for 1,000–2,000 ms within a  $2 \times 2^\circ$  invisible window. During this presaccadic period, probes might be flashed in the RF as discussed in the following *Probe presentation section* (Fig. 1, PRE probes). A saccade target was displayed outside of the neuron’s RF, and the monkey had 500 ms to make a saccade to the target (window:  $\sim 3 \times 3^\circ$ ; saccade period in Fig. 1). A second, postsaccadic period of fixation occurred at this new location (1,000–2,000 ms). This was a second period during which probes might appear in the RF (Fig. 1, POST probes). Finally, to keep the task as similar as possible in both fixation periods, we had the monkey make another saccade to end the trial (not shown); after the second fixation period elapsed, a second saccade target appeared and the monkey made a saccade to it (window:  $\sim 3 \times 3^\circ$ ) within 500 ms. Maintenance of fixation in this window for 200–500 ms completed the trial and resulted in a liquid reward. Breaking fixation, making saccades outside the target windows, or generating late saccades resulted in an aborted trial and no reward. Saccade target positions remained identical within a block of trials, and aborted trials were re-run later in the block.

### Randomized parameters

Two key parameters were randomized on a trial-by-trial basis: the number of probes presented (1 or 2) and when they appeared relative to the saccade (before or after).

### Number of probes: 1st Only, 2nd Only, and Probe Pair trials

Neuronal adaptation is elicited by flashing two probes sequentially and measuring the response to the second probe relative to that of the first probe. Thus to accurately quantify the adaptation, it is important to measure the response to each probe when presented individually. We measured visual responses to individual probes using 1st Only trials (Fig. 1, A and D, 1st Only) and 2nd Only trials (Fig. 1, B and E, 2nd Only). In the test condition for eliciting adaptation, the same two probes appeared sequentially; these were Probe Pair trials (Fig. 1, C and F).

### Probe presentation relative to the saccade: presaccadic versus postsaccadic

In one half of the trials, probes were presented before the saccade (termed PRE trials; Fig. 1, A–C). In the other half, probes were presented after the saccade (POST trials; Fig. 1, D–F). The probe timings were the same in PRE and POST trials except for when the first probe appeared. The PRE trial period began with an initial foveating saccade of random direction and amplitude. To minimize any potential influence of these widely varying saccades on the subsequent visual responses, we delayed onset of the first probe for 200 ms after start of fixation. In contrast, the POST trial period followed a well-controlled, stereotyped saccade (Fig. 1, *middle column*). Here we could more carefully test saccadic influences on visual responses. For POST trials, we timed the first probe to start 30 ms after start of fixation.

For both PRE and POST trials, the onset time of the second probe, when present (i.e., in Probe Pair and 2nd Only conditions), varied according to the particular ISI for a given block (see *Manipulation of ISI*). We timed the events so that, in both the PRE and POST conditions, the second probe appeared long before a saccade (200–600 ms before its onset) to minimize the effects of saccade preparation on our visual responses. The main point of using the two conditions was to determine whether adaptation differed immediately after a saccade (POST condition) in comparison to before a saccade (PRE condition). As will be reported at the start of RESULTS, we found no significant differences in the majority of our data between PRE and POST trials, so for most analyses, PRE and POST data were pooled.

### Manipulation of ISI

The ISI was kept constant within a block of trials and randomly changed between blocks. ISI refers specifically to the amount of time between the offset of the first probe and the onset of the second probe. Six ISIs were examined: 17, 50, 100, 200, 400, and 800 ms. It was not feasible to run the entire range of ISIs for each neuron. On average, we collected full data sets (i.e., all combinations of PRE/POST and 1st Only, 2nd Only, and Probe Pair conditions) for two to four ISIs in each recording session.

### Spatial configuration of the task

Probes were white ( $40 \text{ cd/m}^2$ ,  $0.6 \times 0.6^\circ$ ) and one frame ( $\sim 17 \text{ ms}$ ) in duration presented on a dark background ( $0.8 \text{ cd/m}^2$ ). The fixation point was blue ( $1.2 \text{ cd/m}^2$ ;  $0.3 \times 0.3^\circ$ ), and saccade targets were red ( $0.3 \times 0.3^\circ$ ). To minimize afterimages or low-level adaptation effects (Marlin et al. 1991; Movshon and Lennie 1979), we did not present the two probes at the same location in a given Probe Pair trial. Instead,

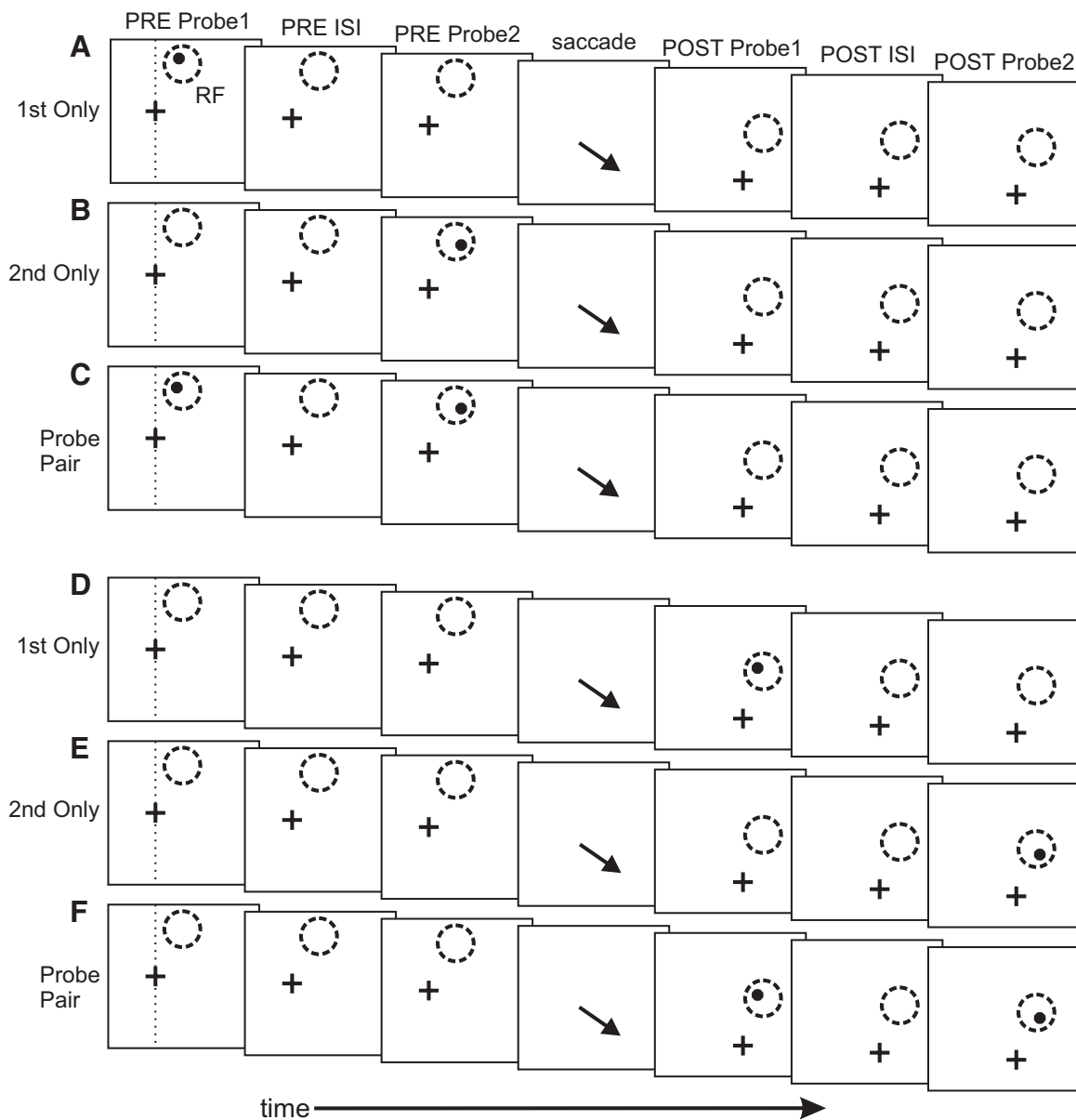


FIG. 1. Layout of the task, progressing from start (left) to finish (right). Vertical dotted line represents the vertical meridian of the visual field and dashed circle represents the neuron's receptive field (RF; neither were visible to the monkey). Each trial began with an initial period of fixation at the center of the screen (cross; leftmost 3 columns), which was followed by a saccade (arrow; middle column) and a 2nd period of fixation (rightmost 3 columns). The trial ended with a 2nd saccade (not shown). Visual probes were presented before the saccade in PRE trials (A–C) and after the saccade in POST trials (D–F). 1st Only (A and D) and 2nd Only (B and E) control conditions used a single probe at times identical to those of the Probe Pair condition (C and F). Probes were never presented both in the PRE and POST periods in the same trial. For clarity of illustration, all stimuli are shown as black, but see text for colors used in the experiment. ISI, interstimulus interval, ranged from 17 to 800 ms.

we gave the probes a small spatial offset. For FEF recordings, probes were spatially offset  $4^\circ$  from each other, symmetrically around the center of the RF; each probe was  $2^\circ$  away from the RF center. For supSC recordings, to account for the smaller diameter RFs, probes were  $1^\circ$  away from the RF center (Cynader and Berman 1972; Wurtz et al. 1980). The axis of the probe offset locations was always orthogonal to the fovea–RF axis to minimize apparent radial motion effects (Xiao et al. 2006).

It is crucial to note that the location of the first presented probe in a pair was randomized between the two offset locations and balanced so that each probe appeared in the first ordinal position for an equal number of trials. Hence if there were any slight differences in visual response or adaptive influence between the two probe locations, our results represented the average. However, quantitative analyses

showed few if any differences. As reported in RESULTS, the two probe locations nearly always elicited identical visual responses.

In all trials, saccades were directed outside of the RF to eliminate any saccade related activity, which is common in FEF neurons (Bruce and Goldberg 1985). RFs and saccade target positions were located contralateral to the recording hemisphere or along the vertical meridian.

#### Recording and data collection

At the start of a recording session, a single tungsten electrode (300 k $\Omega$  to 1M $\Omega$  impedance @ 1 kHz; FHC, Bowdoinham, ME) was lowered through a guide tube (23 gauge) using a custom microdrive system (LSR 2008; details at <ftp://lsr-ftp.nei.nih.gov/lst/StepperDrive/>).

A plastic grid with  $1 \times 1$ -mm hole spacing (Crist et al. 1988; Crist Instruments, Hagerstown, MD) was placed inside the recording chamber to map the topography of the underlying structures. FEF, located along the anterior bank of the arcuate sulcus, was identified as the region in which fixed-vector saccades were evoked  $>50\%$  of the time using low-current ( $<50 \mu\text{A}$ ) microstimulation (Bruce and Goldberg 1985). Superficial SC was identified physiologically by neurons with brisk visual activity and small, topographically arrayed RFs located  $\sim 1$  mm above neurons with broader visuomotor responses in the same structure (Richmond and Wurtz 1980). The characteristic topographic maps for both structures were confirmed with systematic recording and stimulation mapping (Bruce et al. 1985; Robinson 1972). Standard extracellular recording techniques were used to isolate action potentials from single neurons (FEF; Sommer and Wurtz 2000). Electrode stability for recording multiunit activity (supSC) was implemented via continuous on-line waveform inspection.

Once a neuron was isolated, its RF was mapped using an iterative procedure that located the center of the RF in a precise but time-efficient manner. The mapping procedure involved having the monkey make saccades to visual targets at a variety of spatial locations. RFs in both FEF and supSC are, at least roughly, topographically organized across the physical surface of the structures (Bruce et al. 1985; Robinson 1972). Thus the response field location changed only gradually (if at all) during a penetration, so any time we encountered a neuron/multiunit site, we already had a general idea about where its response field should be located. To begin mapping an RF for a neuron, we initially presented a "direction series" of stimuli. A visual stimulus would appear in one of eight directions, spaced by  $45^\circ$  increments around the clock (the cardinal and diagonal directions), at the presumed best amplitude. This series showed the best direction for the neuron; it could be in any of the eight directions, or if the response was equally maximal for two adjacent directions, the best direction would be considered in the middle of those two adjacent directions. Hence our resolution in terms of direction was initially  $22.5^\circ$ . We ran an "amplitude series" in which a visual stimulus appeared at one of eight eccentricities at the best direction to find the best amplitude for the neuron ( $1\text{--}35^\circ$ ). To be thorough, we reran the direction series using the same eight directions but now centered on the confirmed best amplitude (rather than the presumed best amplitude as done on the first pass). We continued this process of iterating between the direction and amplitude series (Sommer and Wurtz 2004) until we were certain that we had found the best direction and amplitude of the neuron (the center of its response field). The physical limits of our display, along with the required spatial configuration of the task, precluded us from using neurons with highly eccentric RFs (centers greater than  $\sim 30^\circ$  peripheral). During the mapping procedure, neuronal activity was monitored on-line using real-time raster plots and histograms.

To characterize the separate visual and movement activity of each neuron, we placed a target at the center of the mapped RF and had the monkey make memory-guided saccades to it (Hikosaka and Wurtz 1983; Mays and Sparks 1980). The memory delay period was 500–1,000 ms, randomized in 100-ms increments (see Sommer and Wurtz 2000 for full details). After mapping the RF and confirming a visual response, we began evaluating the neuron while the monkey performed the main experimental task (as described above; Fig. 1).

Behavioral paradigms and data collection were controlled using the REX real-time system (Hays et al. 1982). Neuronal activity and eye position (Riverbend Instruments, Birmingham, AL) were sampled at 1 kHz, and time stamps of each action potential were saved off-line for further analysis. On average, we collected 15 trials (minimum of 10) for each stimulus arrangement per ISI condition for each neuron. Saccades were detected on-line using velocity criteria and verified off-line using template matching procedures. Saccade start- and end-points were confirmed by the investigator for each trial during analysis.

To provide visual stimulation, the REX system controlled a separate computer with its own graphics card. Once the latter computer was commanded to present a pair of visual probes, it independently timed the ISI with no further input from REX, thereby providing precise probe timings. The stimuli were back-projected by an LCD projector (ViewSonic PJ550, Walnut, CA) onto a tangent screen (Stewart Filmscreen, Torrance, CA) in a dimly lit room. The screen was positioned  $\sim 58$  cm from the monkey's eyes and extended  $\sim 43 \times 38^\circ$  of the horizontal and vertical visual angle, respectively. Screen refreshes and exact stimulus onset and offset times were detected continuously on-line by a photocell circuit. Photocell data were recorded by the behavioral computer and used to correct for the lag as a function of vertical location caused by the rastering of the projector.

### Data analysis

For off-line data analysis, spike trains were transformed to spike density functions (SDFs) by convolution with 3-ms-wide Gaussians (MacPherson and Aldridge 1979). We also tried Gaussians 1–10 ms in width but found that 3 ms best characterized the qualitative effects observed in the raw data. All analyses and figures use 3-ms SDFs unless noted otherwise.

### Penetration

To characterize changes in neuronal activity, our main goal was to measure the first neuronal response and its effect on the strength of the second response. We defined the term "penetration" as a measure of neuronal adaptation. Penetration quantifies the extent to which a neuron responds to a second probe when it is part of a pair compared with when it is presented alone (i.e., not preceded by a 1st probe). In other words, penetration represents whether flashing two visual probes in a row results in a second visual response that is obliterated (0% penetration), moderately potent (0–99% penetration), or as strong as a normal single visual response (100% penetration). For the sake of clarity, we chose to refer to the amount of remaining activity rather than the amount of missing activity of the second neuronal response. In essence, penetration is the inverse of "suppression," which quantifies the extent to which a visual response is squelched. To our knowledge, there is no alternative term in physiology that succinctly describes the magnitude of neuronal activity that remains detectable (or "penetrates") despite the effects of adaptation.

The first step in calculating penetration was to measure the magnitude of the response to a second probe when it was presented as part of the Probe Pair ( $Response_{2\text{pair}}$ ) compared with the response when it was presented in the 2nd Only condition ( $Response_{2\text{alone}}$ ). An initial "uncorrected" measure of penetration was the difference in areas under the  $Response_{2\text{pair}}$  and  $Response_{2\text{alone}}$  SDFs. Specifically, we calculated the  $Response_{2\text{pair}}$  SDF by subtracting the activity contributed by the first probe, as measured in the 1st Only condition, from the activity evoked by the Probe Pair (Fig. 1A, left). A byproduct of this calculation was that it removed baseline activity. The remaining activity represented the response to the second probe of a pair, i.e.,  $Response_{2\text{pair}}$  (Fig. 2B, left). We transformed the visual response to the 2nd Only probe (Fig. 2A, right) into a comparable function,  $Response_{2\text{alone}}$ , by subtracting baseline activity from it (Fig. 2B, right). Baseline activity was measured during initial fixation in a 50-ms window centered on the onset of the first probe.

The next step was to quantify the difference between the visual responses in the  $Response_{2\text{pair}}$  and  $Response_{2\text{alone}}$  SDFs (Fig. 2B, left and right, respectively). The visual response was measured as the area under the SDF within a 10-ms epoch (shorter and longer epochs were tried as well, with little difference in results). The visual response in the  $Response_{2\text{alone}}$  SDF was always clearly identifiable, so we centered the epoch at the peak of this response (Fig. 2C, right, time  $x$ ). In contrast, the visual response in the  $Response_{2\text{pair}}$  data was not as easily identifiable because of the neuronal adaptation effect. One

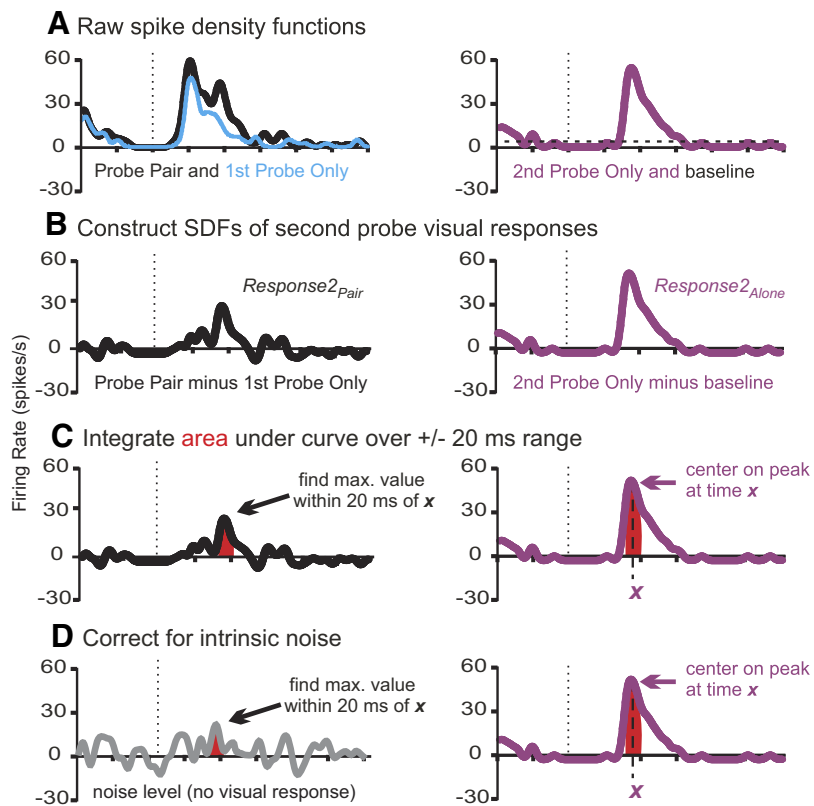


FIG. 2. Illustration of steps used to calculate “penetrance”. *A (left)*: Probe Pair (black) and 1st Probe Only (blue) spike density functions (SDFs). *Right*: 2nd Probe Only SDF (purple) and baseline activity (black dashed line). Gray vertical dashed lines indicate time of first probe onset. *B (left)*: Response<sub>2\_Pair</sub> SDF obtained by subtracting the 1st Probe Only SDF from the Probe Pair SDF. *Right*: Response<sub>2\_Alone</sub> SDF obtained by subtracting baseline activity from the 2nd Probe Only SDF. *C*: integration of area (red) in the response epoch of (left) the Response<sub>2\_Pair</sub> SDF and (right) the Response<sub>2\_Alone</sub> SDF. *D*: intrinsic noise SDF (gray, left) used to determine background penetrance relative to the full Response<sub>2\_Alone</sub> epoch (right). Each tick mark on the abscissa represents 100 ms.

simple way to address the response ambiguity would be to center the Response<sub>2\_Pair</sub> epoch at the same time as the Response<sub>2\_Alone</sub> epoch, i.e., at time  $x$ . However, we were concerned that the Response<sub>2\_Pair</sub> visual response could be slightly offset in latency from the Response<sub>2\_Alone</sub> visual response. That is, it seemed possible that a preceding stimulus could affect visual latency as well as magnitude. To compensate for potential shifts in latency, we varied the Response<sub>2\_Pair</sub> epoch relative to the Response<sub>2\_Alone</sub> epoch (over  $x \pm 20$  ms) until the area under the Response<sub>2\_Pair</sub> visual response was maximal (Fig. 2C, left). Next, we subtracted the two areas (Response<sub>2\_Alone</sub> visual response  $-$  Response<sub>2\_Pair</sub> visual response) to yield a differential visual response in units of spikes per second. This value was transformed to a percentage of the single-probe visual response of the neuron under study, so that we could use this normalized value to compare adaptation between neurons that may have widely varying visual responses. (To quantify the single-probe visual response, we repeated the above calculations, but compared the 1st probe only SDF to a segment of the SDF far from the visual response.) The differential visual response was expressed as a percentage of the single-probe response to yield the “uncorrected penetrance.”

For penetrance to have useful meaning, it should be zero if a visual response was completely absent in the Response<sub>2\_Pair</sub> curve. However, our algorithm is agnostic as to whether a visual response occurs in Response<sub>2\_Pair</sub>, and so it necessarily finds the maximum positive area under this SDF over the range  $x \pm 20$  ms, regardless of whether it is caused by the second probe or noise. The end result is that uncorrected penetrance cannot reach zero. Our next goal was to adjust for this analytical artifact and obtain a full range, 0–100%, penetrance metric. To this end, we found the actual minimum level, or “intrinsic penetrance,” by calculating penetrance values with test curves having identical noise characteristics but known to lack a second visual response. We constructed such curves using the 1st Only trials. For each neuron, half of the 1st Only trials were randomly selected, pooled, and transformed into a SDF. The same procedure was used for the other half of the 1st Only trials. The difference between the two

SDFs eliminated the visual response but retained the inherent noise level (Fig. 2D, left). This differential SDF was used as a stand-in for the Response<sub>2\_Pair</sub> data and was subtracted from the Response<sub>2\_Alone</sub> data (Fig. 2D, right) to calculate the intrinsic penetrance of the neuron. We found that the average intrinsic penetrance (solely attributable to noise fluctuations) was  $\sim 24\%$  for FEF. Using this as the lower bound for uncorrected penetrance values, the values were rescaled to a final corrected value in which 0% represents no visual response. “Penetrance,” as used for the remainder of this paper, will refer to this final corrected value.

#### Normalization of population data

To account for variations in intensity of visual responses between neurons when compiling the population graphs of Fig. 4, we normalized each neuron’s responses to the maximum firing rate in the visual response epoch (50–150 ms after stimulus onset) for the 1st Only PRE condition for each neuron at every ISI. The neuron’s entire SDF was divided by this maximal response, and visual activity across all neurons for a given ISI was averaged to get the final normalized population response. For Fig. 4, B and C, the normalized 1st Only response was subtracted from the normalized Probe Pair response to obtain the residual second probe response traces. The maximal response (Probe Pair responses in Fig. 4A, residual second probe responses in Fig. 4, B and C) was normalized to 1.0 and the remaining activity scaled accordingly.

#### Saccade direction versus penetrance

To look for a relation between impending saccade direction and penetrance, we normalized the saccade target positions relative to probe position in polar coordinates. Zero degrees equaled a direct saccade to the probes and 180° represented a saccade in the diametrically opposite direction. Saccade directions from opposite hemispheres were converted to this 0–180° scale. Using this scale, we

analyzed whether penetrance varied with saccade direction, as described in RESULTS.

### Sigmoid fits

Best-fit lines and three-parameter sigmoid curves (Fig. 6) were determined using SigmaPlot 10.0 software package (Systat Software, San Jose, CA). The preferred model (linear vs. sigmoidal) was determined by calculating the Akaike information criterion (AIC) (Akaike et al. 1998; Sakamoto et al. 1986). AIC uses the residual sum of squares and adds a penalty for additional parameters to deter overfitting the data. A lower AIC value indicates a more appropriate model.

### Constructed multiunit FEF responses

To estimate whether our approach of recording single neurons in FEF and multiple neurons in supSC may have affected the comparative penetrance values between the two areas, we created “virtual” multiple neuron recordings from our single neuron FEF data. We combined FEF responses into multiunit-like groups by randomly assigning individual FEF neurons into groups of two or three. This number of neurons per group matched our estimate of the number of neurons isolated per site in the supSC recordings. FEF group SDFs were combined according to ISI and averaged before recalculating penetrance values.

### Postsaccadic suppression index

We qualitatively observed a postsaccadic suppression effect in the visual responses, and we quantified this effect by measuring the number of spikes occurring in 1st Only trials during the visual response epoch (50–150 ms after stimulus onset) for PRE versus POST conditions. The total number of spikes was compared before (PRE) and after (POST) the initial saccade using a suppression index of the form  $(FR_{pre} - FR_{post}) / (FR_{pre} + FR_{post})$ , where FR indicates firing rate during the response epoch. Index values ranged from  $-1$  to  $1$ , corresponding to relatively facilitated and suppressed POST responses, respectively.

### Latency of neuronal responses

The onset latency of visual activity was estimated using a running, paired  $t$ -test that compared the average firing rate in a  $\pm 15$ -ms interval fixed and centered at stimulus onset ( $-15$  to  $15$  for the first probe and  $ISI \pm 15$  ms for the second probe, both relative to first probe onset), with average firing rates in a sliding interval of the same duration but advanced in 1-ms intervals. Significant visual activity was defined as periods of activity where  $P < 0.01$  for  $\geq 10$  ms. We designated the first significant point in this period as the neuron's latency.

We confirmed the accuracy of our latency values by comparing them with values obtained using a second, simpler method that used the peaks of neuronal activity as temporal landmarks. We determined the response latency of the first peak in a pair using data from the raw Probe Pair SDF. To determine the latency of the second peak in a pair, we used the Probe Pair minus 1st Only condition ( $Response2_{pair}$ ) SDF. All analyses were conducted in conjunction with visual inspection of histograms and raster plots to ensure accuracy. Latencies determined by the two methods ( $t$ -test and peaks) were highly correlated and not significantly different in either FEF or supSC (rank sum test,  $t$ -test vs. peaks, FEF:  $P = 0.982$ , supSC:  $P = 0.984$ ; regression of  $t$ -test vs. peaks, FEF:  $r = 0.994$ ,  $P < 0.001$ , supSC:  $r = 0.999$ ,  $P < 0.001$ ).

## RESULTS

Our central hypothesis was that sequential visual stimuli would result in adaptation of visual responses in FEF neurons.

Moreover, because FEF is polysynaptically removed from the retina, we predicted that the adaptation would be stronger than that in the retinally recipient supSC. We tested these ideas by presenting two consecutive visual stimuli separated by various durations (17–800 ms) and recording the neuronal responses in FEF and supSC. Responses to individual probes (1st Only or 2nd Only) were recorded as controls. We studied 40 single, visually responsive neurons in FEF (*monkey K*: 20, *monkey N*: 11, *monkey C*: 9) and, for comparison, 14 multiunit sites in supSC (*monkey K*: 11, *monkey M*: 3).

### Decreased second response to Probe Pair

**SINGLE NEURON EXAMPLE.** We found that neuronal adaptation is strong in FEF neurons. Data from a single FEF neuron are presented in Fig. 3. Flashing a single, brief-duration probe in a neuron's RF (1st Only condition; Fig. 3, *middle row*) yielded a characteristic increase in the rate of activity—a visual response—beginning  $\sim 60$  ms after stimulus onset. Flashing an identical single probe later in fixation (2nd Only condition; Fig. 3, *bottom row*) elicited similar visual responses. Hence all of the visual stimuli used as probes elicited robust visual responses when presented singly.

On the other hand, strong visual responses were not always seen for probes presented doubly, i.e., in the Probe Pair experimental condition. The *top row* of Fig. 3 shows the response of a typical FEF neuron to two sequential probe stimuli presented using three ISIs (50, 100, and 400 ms). Similar to the 1st Only condition (*middle row*), visual responses to the first probe at all three ISIs were strong. However, the response to the second probe could be diminished. Given the identical spatial and temporal aspects of probe presentation in the single and pair conditions, it was evident that decreased responses to the second probe of a pair were caused by the immediately preceding first probe.

At the shortest interval for this neuron ( $ISI = 50$  ms), the presentation of the second probe elicited a negligible visual response (Fig. 3, *top left*). At best, the second probe at  $ISI = 50$  ms caused a slight bump in the ongoing response to the first probe. When the time between the probes was increased by 50 ms at  $ISI = 100$  ms, the response to the second stimulus increased to an intermediate level, eliciting roughly one half of the typical visual response (Fig. 3, *top center*). Finally, when the probe pair stimuli were separated by 400 ms, the neuron displayed two equivalent responses, as if responding independently to each of the single probes (Fig. 3, *top right*). These ISI-dependent alterations in visual responsiveness to second probes were quantified using our penetrance metric. For this example neuron, the second probe of the Probe Pair exhibited penetrance levels of 3% at  $ISI = 50$  ms, 49% (about half-recovery) at  $ISI = 100$  ms, and 112% (slightly more than full recovery) at  $ISI = 400$  ms. Thus the amount of adaptation in the second visual response was a function of time between the first and second visual stimulus.

The example neuron of Fig. 3 shows data collected in the PRE condition (see Fig. 1). Data for this neuron in the POST condition were similar. We tested every neuron in both the PRE and POST conditions to compare adaptation effects before and immediately after a saccade. We found no significant differences between ISI-dependent adaptation in the PRE and POST conditions in either the FEF or the supSC samples (2-way ANOVA on penetrance with ISI and PRE/POST as factors; FEF:  $P = 0.259$ ,

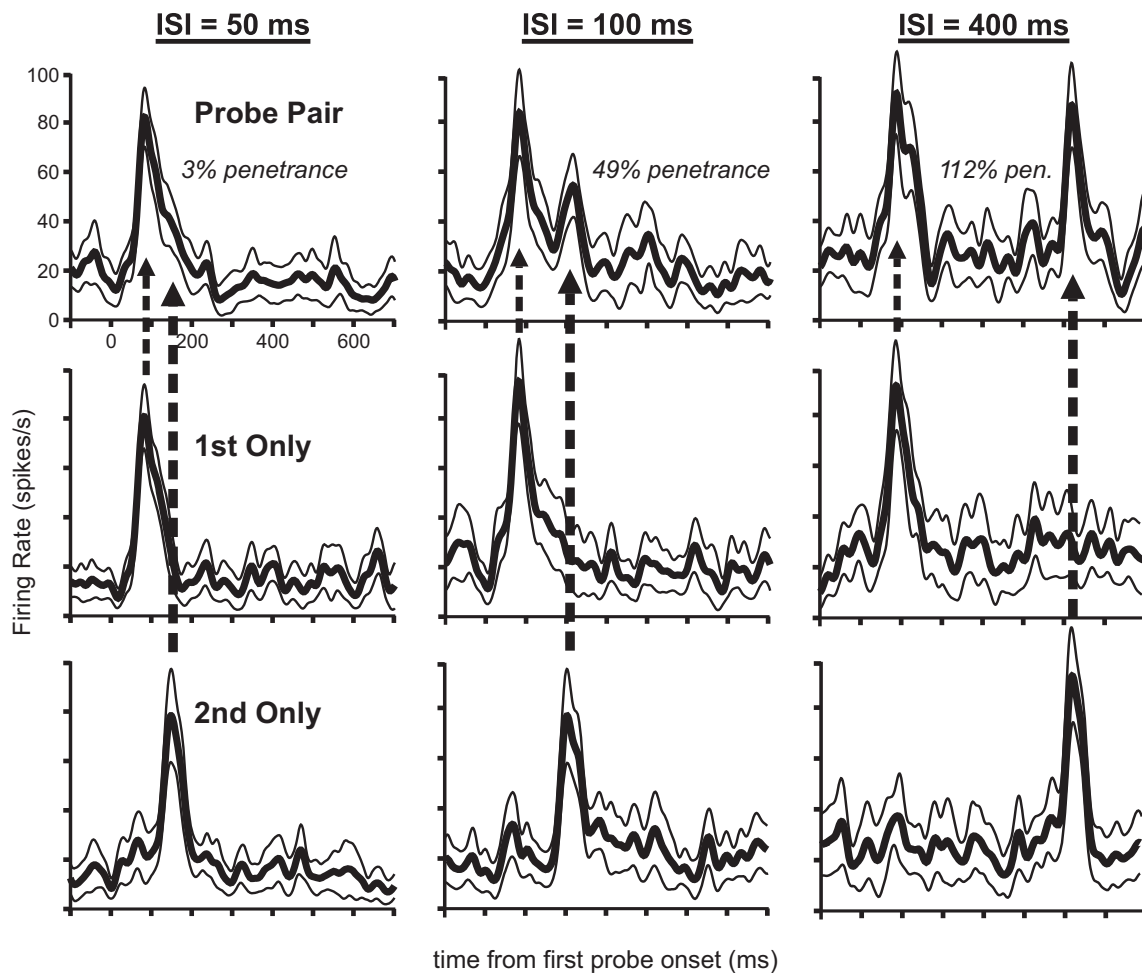


FIG. 3. Example visual responses from a single frontal eye field (FEF) neuron. *Top row*: Probe Pair condition. *Middle row*: 1st Only condition. *Bottom row*: 2nd Only condition. The three columns show results of using ISIs of 50, 100, and 400 ms. Dashed arrows relate timings of corresponding visual responses across rows. SDFs depict means (bold lines) and SE (thin lines).

supSC:  $P = 0.710$ ). For the rest of this paper, we pool the PRE and POST data, unless noted otherwise.

To minimize lower-level adaptation effects (e.g., originating in the retina), we positioned the two probes near the RF center but with a slight spatial offset from each other. One concern was that the two probe locations may have yielded different visual responses. We tested this possibility in a subset of FEF neurons (18 of 40) and for all supSC multiunit groups. The visual responses were rarely different at the two probe locations ( $t$ -test: a single FEF neuron was significant at  $P = 0.016$ ; a single supSC multiunit group was significant at  $P = 0.022$ ). The sequence of probe presentations also did not matter; the results were similar regardless of which probe appeared first ( $t$ -test: a single FEF neuron was significant at  $P < 0.001$ ; there were no significant supSC multiunit groups). As an extra safeguard, we randomized the order of probe presentation so that each of the two probe locations was presented first on half of the trials. Because of this randomization, any differences in visual responses at the spatially offset probe locations could not have influenced our results.

#### Population results

To show the overall adaptation effect in a qualitative manner, we constructed population averages of FEF neuronal

activity (Fig. 4A). The firing rate of each neuron was normalized to its maximal response, and the normalized SDFs were averaged for each ISI. As expected, the visual response to the first probe of a probe pair was indistinguishable between ISIs (Fig. 4A, arrow). The visual response to the second probe of a probe pair, however, increased as ISI increased (Fig. 4A, 2nd visual responses are marked with dots).

We were able to extract the visual response to the second probe at each ISI using the population responses to single and double probe conditions. In Fig. 4B, the response to the 1st Only probe was subtracted from the response to the Probe Pair, for each neuron at each ISI, leaving the residual response to the second probe of the pair. This format allows one to appreciate the magnitude of the adapted second probe responses relative to the baseline noise level of activity across the full range of ISIs (17–800 ms).

As Fig. 4B shows, visual responses to the second probe are discriminable from the noise level even at the shortest ISIs where responses to the first and second probes overlap and absolute responses to the second probe are small. As suggested by the single cell example in Fig. 3, in the population activity, there is a gradual increase in the response to the second probe with increasing ISI (Fig. 4B). Full visual responses to the second probe were observed at ISI = 400 ms in the population.

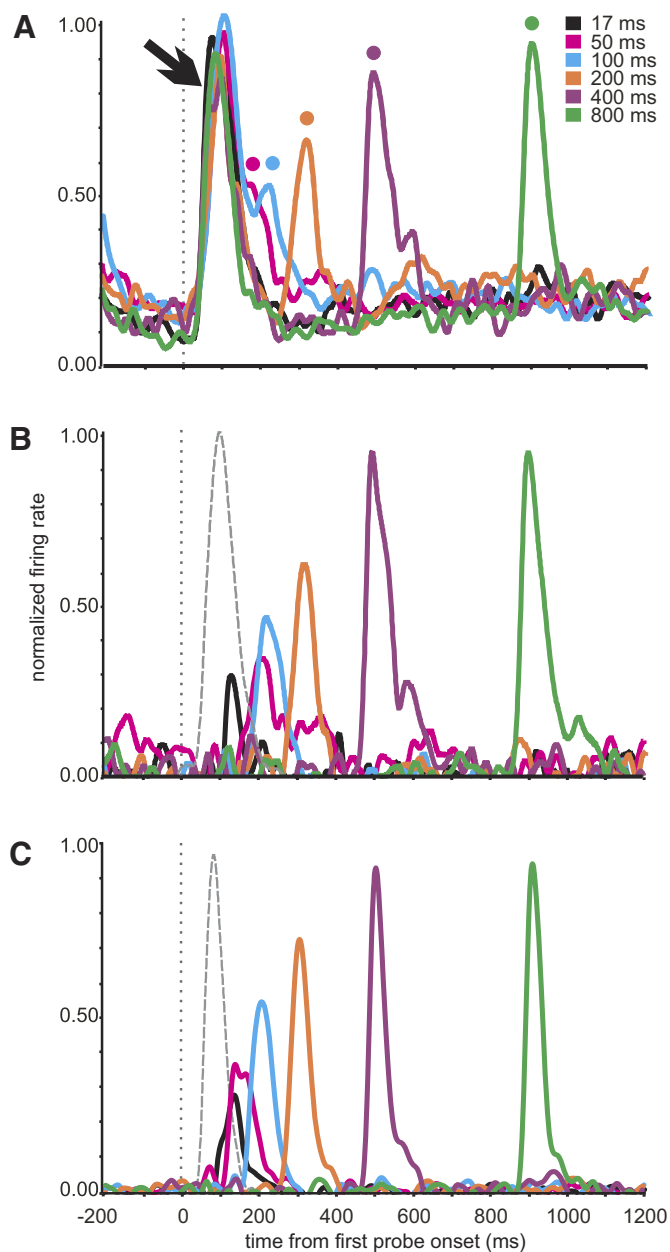


FIG. 4. *A*: normalized visual responses to Probe Pair at each ISI in the FEF population. Vertical dotted line indicates time of first probe onset. Arrow shows main response to first probe; dots label clear responses to second probes. The dot for ISI = 17 ms (not shown) is obscured by the first probe responses. *B*: normalized, baseline-corrected, extracted visual responses to the second probe of Probe Pairs in the FEF population. Responses to first probes, in 1st Only trials, were subtracted from the data in *A* so that only the responses to second probes remained. For reference, the gray dashed curve represents a typical response to a first probe (similar for all ISIs). SDFs used 10-ms-wide Gaussians for illustration purposes. *C*: superficial superior colliculus (supSC) population responses. Same format as in *B*.

We also used ISI = 800 ms to ensure that the return to responsiveness was not a temporary reprieve. Responsiveness at 400- and 800-ms ISIs were comparable, suggesting that the time course of adaptation is completely finished after an ISI of 400 ms. The same effect was seen in the supSC population responses (Fig. 4C).

To formally quantify the population data, we calculated the average penetrance at each ISI. For FEF (Fig. 5, black

bars), the mean penetrance values as a function of ISI matched what was observed qualitatively in the population responses (Fig. 4B). Penetrance increased with ISI and reached ~100% at 400 and 800 ms. This effect was highly significant (1-way ANOVA,  $P < 0.001$ ). Further analysis showed that ISI-normalized penetrance did not vary as a function of baseline activity (Pearson correlation;  $P = 0.430$ ), RF eccentricity (Pearson correlation;  $P = 0.675$ ), or the direction of the impending saccade (Pearson correlation;  $P = 0.259$ ; see METHODS).

#### Comparison of effects in FEF versus supSC

To compare neuronal adaptation at different points along the neuraxis, we recorded neuronal activity in supSC (see METHODS) and calculated penetrance values in an identical manner. Previous studies found neuronal adaptation effects in supSC using similar tasks (Dorris et al. 2002; Fecteau et al. 2004; Robinson and Kertzman 1995; Wurtz et al. 1980). supSC is a midbrain structure located one synapse away from retinal input. Thus it provides an important contrast to FEF in pre-frontal cortex that receives no direct retinal input. Because of its close proximity to the retina, one might expect supSC to exhibit less adaptation than FEF.

supSC showed the same general adaptation effect as FEF (Fig. 5, gray bars). Like FEF, supSC showed diminished responses at the shortest ISIs but relatively full visual responses when ISI  $\geq 400$  ms. For our supSC data, as with our FEF data, the change in penetrance as a function of ISI was highly significant (1-way ANOVA,  $P < 0.001$ ).

Neuronal adaptation in both FEF and supSC showed comparable adaptation at corresponding ISIs, but were there significant differences in the effect between the structures? To answer this question, we performed a two-way ANOVA on penetrance using ISI and FEF/supSC as factors. We found a significant main effect of brain area ( $P < 0.001$ ). The supSC generally showed higher penetrance (less adaptation) at each ISI compared with FEF (Fig. 5).

We next analyzed whether the differences between FEF and supSC were caused by differences in the rate of adaptation (e.g., FEF and supSC showing similar adaptation at short ISIs but differing at long ISIs) or by differences in overall adaptation (e.g., supSC showing uniformly higher adaptation across ISIs). We determined the best-fit linear regression for both the FEF and supSC penetrance values over the range of ISIs where

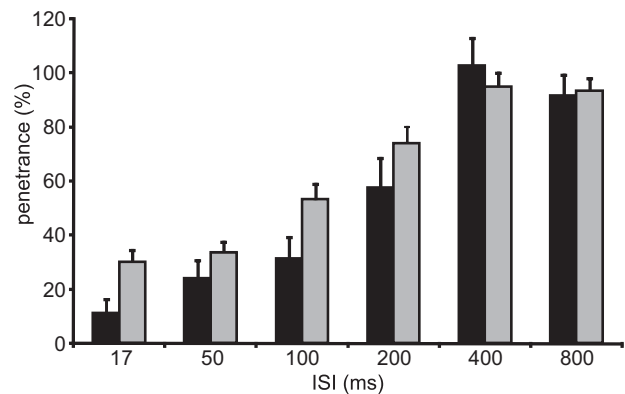


FIG. 5. Mean penetrance values with SE bars for FEF (black) and supSC (gray) populations at each ISI.

penetrance changed (ISI = 17–200 ms; ISIs of 400 and 800 ms were excluded because their ceiling penetrance values would inappropriately skew the linear regression.) In agreement with the population statistics, we found that the linear regressions were significantly different between FEF and supSC (*F*-test of regressions; FEF:  $y = 0.239x + 5.036$ , supSC:  $y = 0.252x + 20.267$ ;  $P < 0.001$ ; Glantz 2002). This difference in regressions was not caused by a difference between slopes ( $P = 0.876$ ) but rather to a highly significant difference between *y*-intercepts ( $P < 0.0001$ ; Glantz 2002). The difference cannot be attributed to contrasting noise levels in FEF and supSC because our penetrance metric accounted for such potential inequalities (see METHODS). In sum, the rate of neuronal adaptation across ISIs was consistent between FEF and supSC, but the overall level of adaptation differed significantly between the two structures.

To obtain a heuristic description of the difference in adaptation between FEF and supSC and to facilitate comparisons of adaptation in other brain areas in the future, we calculated the ISI required to elicit 50% penetrance. We determined this ISI value by fitting sigmoid curves to the penetrance versus ISI data. Over the entire ISI range, sigmoids provided a better fit than linear regression as determined by lower AIC values (FEF: AIC = 1090.8 for a sigmoid curve and 1107.3 for a linear fit; supSC: AIC = 622.1 for a sigmoid curve and 654.7 for a linear fit). We plotted penetrance values for all FEF and supSC neurons and fit the resulting scatterplots with three-parameter sigmoid functions (Fig. 6, *A* and *B*, respectively). The ISI values needed for half penetrance were 163 ms in FEF and 97 ms in supSC (Fig. 6*C*, dashed vertical lines). The separation between the 95% CIs of the data from the two structures at the 50% penetrance level (Fig. 6*C*, thin lines) indicated that the ISI values at half penetrance (163 and 97 ms) were significantly different.

Despite the nearly identical results between our multiunit supSC recordings and previous single-unit experiments (Robinson and Kertzman 1995; Wurtz et al. 1980), it was possible that the difference in FEF and supSC penetrance values was related to differences in our data collection because we recorded single neurons in FEF but multiple neurons in supSC. We found it difficult to maintain isolation of single supSC neurons for long enough to collect full data files, so we allowed our supSC data to consist of approximately two to three simultaneously recorded single neurons (i.e., multiple single units). It seemed unlikely that this difference would affect penetrance calculations, but to test this hypothesis, we used our FEF data to create posthoc multiunit responses by randomly placing each single-unit FEF response into groups of two to three neurons (see METHODS). Combining single neurons into small multiple single unit groups had no effect on the population penetrance values for FEF (2-way ANOVA,  $P = 0.808$ ). Therefore the differences between penetrance in FEF and supSC likely represent true differences in duration-dependent responses between areas rather than artifacts of single versus multiple neuron recordings.

#### Influence of saccade generation on neuronal adaptation

A wealth of psychophysical research suggests that our perception of time is distorted just before and after an eye movement. Specifically, estimates of temporal duration show a

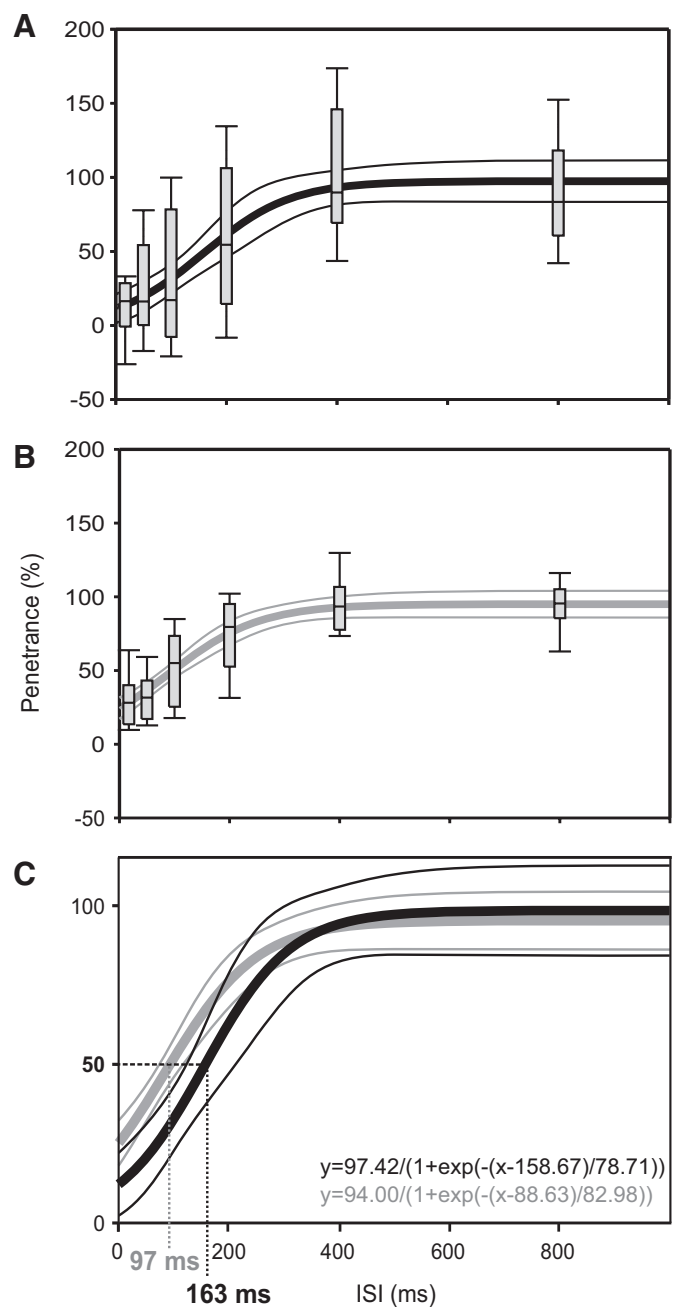


FIG. 6. Three-parameter sigmoid fits (thick lines) and box-whisker plots of (*A*) FEF and (*B*) supSC data. Box-whisker plots show median (line), 25th and 75th percentiles (box), and 10th and 90th percentiles (error bars). Thin lines represent 95% confidence bands. *C*: overlay of FEF (black) and supSC (gray) sigmoid fits from *A* and *B*. Vertical dashed lines indicate the ISI necessary to elicit 50% penetrance. Equations for the sigmoid fits are at *bottom right*.

systematic decrease before a saccade and an increase just after a saccade (Georg and Lappe 2007; Matin et al. 1972; Morrone et al. 2005; Yarrow et al. 2001). It is possible that these perceptual distortions around the time of eye movements are reflected in the corresponding visual activity in FEF. Adaptation changes over time (Fig. 4), and therefore changes in visual response magnitude might provide information about the timing of sequential stimuli. However, the perceptual distortions seen in psychophysical studies suggest that the latency of neuronal processing fluctuates perisaccadically. The most straightforward

hypothesis is that some mechanism accelerates or delays visual processing in areas underlying conscious vision, such as prefrontal cortex. Such shifts in latency have long been suggested as a possible correlate of spatial attention in psychophysical studies (Carrasco and McElree 2001; Stelmach and Herdman 1991; Titchener 1908), although to date there is relatively little physiological data to support the claim.

We therefore measured the latency of individual FEF neurons' visual responses to probe pairs at each ISI (see METHODS) and plotted the resulting difference in response onset [response onset asynchrony (ROA)] and stimulus onset [stimulus onset asynchrony (SOA)]. SOA was used instead of ISI because we could not as easily measure the offset of the first neuronal response, as the neuronal analog of ISI would require. Given the proximity of individual probes to the saccade—the second probe presaccadically and the first probe postsaccadically—we might expect altered ROA values that are inconsistent with the actual probe pair intervals. However, we found only one significant inconsistent ROA value (ROA = 202 @ SOA of 217 ms; 2-way *t*-test,  $P = 0.047$ ), and this mismatch was not confirmed using an alternate method that focused on the peak of the visual response (see METHODS). In sum, despite the large changes in the adaptation of visual responses with ISI, the latencies of visual responses were accurate as a function of ISI. supSC response latencies were similarly accurate.

To verify this result, we analyzed the influence of an impending saccade on visual responsiveness on a trial-by-trial basis. We ranked individual trials according to saccadic reaction time and normalized the visual responses (see METHODS). We tested if the time of an upcoming saccade had a significant effect on presaccadic visual activity. This analysis showed no significant correlation ( $P = 0.167$ ). This should not be considered surprising, given the relatively large amount of time between second probe offset and saccade onset, even at the shortest configuration (200–600 ms for ISI = 800 ms).

We did find one clear influence of saccades on our visual responses. It was obvious from inspection of our data that, just after a saccade terminated, visual responses were suppressed. To quantify this “postsaccadic suppression” effect, for each neuron, we compared the 1st Only visual response in PRE trials (where the stimulus was presented ~200 ms after the initial foveating saccade), with the 1st Only response in POST trials (where the stimulus was presented only ~30 ms after saccade termination). We calculated a suppression index to quantify the range of suppression in all neurons (see METHODS and Fig. 7). We found a significant positive shift in the distribution of index values, indicating relatively diminished visual responses after the saccade in both FEF and supSC (1-sample *t*-test, null hypothesis = 0; FEF:  $P < 0.01$ , supSC:  $P < 0.05$ ). The mean index values in both structures were similar (FEF: 0.1281; supSC: 0.110), and the distribution of the two samples did not differ significantly (*t*-test,  $P = 0.804$ ). Reanalysis of the data after removing any sign of correcting or “catch-up” saccades did not affect the results. It should be noted that this suppression affected visual responses to first probes in both the Probe Pair and 1st Only conditions, so when the latter data were subtracted from the former data in our penetrance analyses, the effect washed out. In sum, our data suggest that saccadic eye movements have a lingering suppressive effect on visual responses that continues at least until ~30 ms after the end of the eye movement.

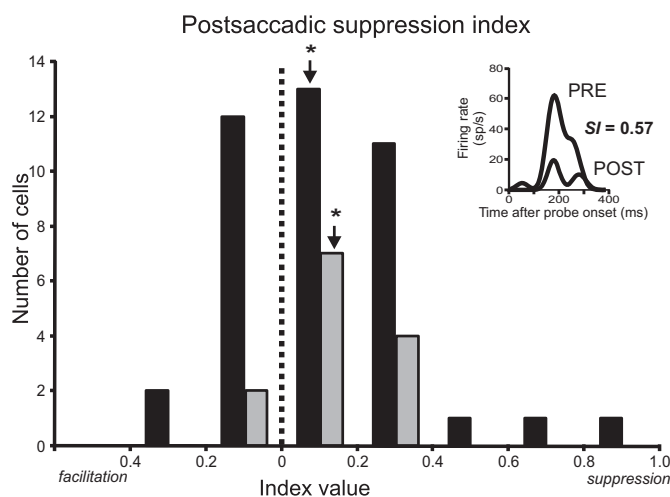


FIG. 7. Distribution of postsaccadic suppression index values for FEF (black) and supSC (gray). Index values were placed into bins 0.2 units wide. Arrows indicate means of the distributions and stars indicate statistical significance ( $P < 0.05$ ; see text for details). Inset: example visual responses to PRE (larger amplitude) and POST (smaller amplitude) 1st Only conditions, showing a neuron with a suppression index value of 0.57. (This particular neuron had a slight biphasic response to the single visual stimulus, especially in the POST condition.)

## DISCUSSION

We characterized neuronal responses to sequential visual stimuli in FEF and, for comparison, supSC. After quantifying neuronal adaptation as a function of ISI, we analyzed differences between the two structures. Finally, we examined the influence of saccade generation on the magnitude and latency of paired visual responses. We found that, in FEF, the second stimulus of a pair evokes a meager visual response at short ISIs (<100 ms). This response increases with ISI until ~400 ms, where it reaches a normal level. The effect is identical in supSC except for a significant increase in responsiveness across ISIs. The major influence of saccade generation is that, in both structures, visual responses are reduced postsaccadically, confirming the time course of psychophysical results (Diamond et al. 2000).

### Adaptation in the visual stream

This study provides the first systematic analysis of neuronal adaptation in an area of prefrontal cortex, namely FEF. Near the other end of the neuraxis, recordings of ON responses in the LGN and optic tract consistently show a return to full responsiveness at ISIs  $\approx 100$ –200 ms (Coenen and Eijkman 1972; Fehmi et al. 1969; Schiller 1968). This ISI is nearly one half of that required for full responses in FEF, suggesting that adaptation in latter areas is not solely attributable to antecedent visual processing. Additionally, the spatial offset of our visual probes precludes a trivial transfer of adaptation entirely from the earliest visual structures. The two probes of a probe pair were close enough in space to activate the RFs of single neurons in FEF but were likely too far apart to activate the RFs of single retinal, LGN, or V1 neurons (although transfer from, say, V4 or IT is possible). A simple explanation is that FEF contributes to the temporal filtering of visual stimuli. Further experiments are needed to determine how much (if any) FEF adaptation occurs de novo, as it seems to do in other visual cortical areas, such as middle temporal cortex (MT) (Priebe et al. 2002).

Surprisingly, comparable temporal studies of neuronal activity in frontal cortex are much less prevalent. Despite the clear importance of understanding the timing of sequential visual responses, relatively few experiments in visual cortex have used simple stimuli at varying intervals and quantified the resulting activity. In V1, Judge et al. 1980a showed that two full visual responses can be elicited once flashed stimuli are separated by ~500 ms (but see also Muller et al. 1999 for longer intervals). Recent work in area V4 also suggests a return to full responsiveness at ISIs ~400–500 ms (Motter 2006). Despite the range of stimuli and procedures used in previous work, our FEF results are generally in accordance with data collected in comparable areas of visual cortex.

Testing supSC neurons in addition to FEF neurons provided us with a critical reference point for incorporating our data within the broader context of adaptation studies. Importantly, our results concur with previous research in supSC (Robinson and Kertzman 1995; Wurtz et al. 1980). Robinson and Kertzman (1995) used a task with cue and target presentation in the RF at varying ISIs, similar to our Probe Pair paradigm. In their single neuron data, they found a return to full responsiveness at ISI  $\approx$  400 ms, matching our multiunit supSC data. Likewise, Wurtz et al. (1980) presented stimuli in the RF at various ISIs to study visual interactions around the time of eye movements. When the longer duration stimulus was presented first, the mean percent response (i.e., ~penetrance) at 200 ms—the longest ISI tested—was ~70% in single supSC neurons, nearly identical to our reported value of 74% penetrance at the same ISI. The tight agreement between previous studies and our data suggests that adaptation in supSC is now well characterized and strengthens our confidence in the accuracy of our FEF results.

### Neuronal coding and mechanisms

We propose that synaptic short-term plasticity (STP) may be important for the observed adaptation effect. STP involves a transient decrease in synaptic strength based on the frequency of neuronal activity (Fortune and Rose 2001; Zucker 1989). STP is governed by calcium-dependent release of neurotransmitter, which, in turn, is limited by the rate at which the available pool of calcium replenishes. The initial large response and subsequent diminished response in neuronal adaptation may therefore be explained by the initial release and firing-during-refilling of calcium stores in the neuron. Thus because adaptation in supSC seems to last nearly twice as long as that of LGN, our results generate the testable hypothesis that recovery from STP is particularly fast in LGN relative to other retinal-recipient visual structures.

Although STP in early visual areas must cause some of the adaptation observed in FEF, it cannot account for all of the FEF adaptation in our study, because of the spatial offsets we used when presenting paired stimuli. The offsets were small relative to the size of a RF in FEF but large relative to the size of a RF in areas such as LGN and striate cortex. In early visual areas, one set of neurons would be activated by the first stimulus of a pair, and a different set of neurons by the second stimulus, so STP-mediated adaptation as described above would seem unlikely. It could be that lateral inhibition in early visual areas (Hartline et al. 1956; Ratliff 1972) also contributes to FEF adaptation. However, we suggest that STP in FEF itself,

and in other extrastriate areas with relatively large RFs, is a more parsimonious explanation. Intracellular work, for example in slices, would likely be needed to test these hypotheses.

One open question is, does adaptation serve a purpose? Neuronal adaptation may function as an efficient means of coding the novelty of incoming visual information (Ringo 1996; Wark et al. 2007; Wiggs and Martin 1998). In this schema, repeated stimulation by identical stimuli leads to a “normal” first response followed by interval-dependent diminished responses that decrease to a plateau (Mayo 2007). Indeed, visual responses in V4 and IT—areas with direct connections to FEF (Schall et al. 1995; Ungerleider et al. 2008)—have shown precisely this phenomenon (Li et al. 1993; Motter 2006; Xiang and Brown 1998). However, because FEF neurons are relatively insensitive to stimulus features (Mohler et al. 1973), it is likely that neuronal adaptation in FEF functions more as a general detection mechanism (likely in the service of eye movements) than a specialized form of short-term object memory as found in IT.

### Perception and inhibition of return

If spatial attention were automatically drawn to the probes, we would expect to see a firing pattern in line with psychophysical data on inhibition of return (IOR; for review, see Klein 2000). Specifically, we would see a higher firing rate at the shortest ISIs because of increased attentional discriminability (Bushnell et al. 1981; Spitzer et al. 1988). We observed some evidence for this effect because initial visual responses (Fig. 4A, arrow) tended to be larger for shorter ISIs (17–100 ms) because of summation of the first and second visual responses in the raw data. In this sense, our data are consistent with previous IOR-related SC results (Fig. 4A) (Dorris et al. 2002; Fecteau and Munoz 2005; Fecteau et al. 2004). This slight amplification of raw firing rate notwithstanding, second visual responses at short ISIs were severely adapted, as shown by subtracting the time-matched single-probe visual responses (Fig. 4B).

Our neuronal data also dovetail with a previous study that measured the neuronal correlates of perceptual awareness in FEF (Thompson and Schall 1999). In that experiment, visual stimuli were presented in the RF at very short ISIs; a target was followed 0–50 ms later by a masking array. Consistent with our data, in that study the first visual response to the target was normal, whereas the second response to the stimulus in the array tended to be weak. Our quantification of neuronal adaptation in FEF could explain the diminished second-stimulus responses seen by Thompson and Schall (1999).

### Future directions

By characterizing the “baseline” activity of FEF visual neurons to sequential stimuli, we open an avenue for future research into the effects of eye movements on stimuli presented just before and after the saccade and accompanying temporal illusions (Georg and Lappe 2007; Matin et al. 1972; Morrone et al. 2005; Yarrow et al. 2001). If such perceptual distortions could be shown in an animal model, the activity of single neurons could be monitored while these illusions occur. We believe that FEF is a promising brain region in which to study these phenomena. FEF is relatively feature-independent

(Mohler et al. 1973) and connected to subcortical structures such as the basal ganglia and cerebellum (Alexander et al. 1986; Lynch et al. 1994; Stanton et al. 1988)—areas thought to play critical roles in timing (Ivry and Spencer 2004; Jahanshahi et al. 2006; Matell and Meck 2004). Finally, FEF is a critical component of the oculomotor circuit needed to maintain transsaccadic spatial stability (Sommer and Wurtz 2002, 2006). It may be that this same pathway assists in maintaining temporal stability before and after eye movements (Yarrow et al. 2004).

#### GRANTS

This research was supported by the Alfred P. Sloan foundation and National Eye Institute Grant R01-EY-017592.

#### REFERENCES

- Akaike H, Parzen E, Tanabe K, Kitagawa G. *Selected Papers of Hirotugu Akaike*. New York: Springer, 1998, p. viii.
- Alexander GE, DeLong MR, Strick PL. Parallel organization of functionally segregated circuits linking basal ganglia and cortex. *Annu Rev Neurosci* 9: 357–381, 1986.
- Baylis GC, Rolls ET. Responses of neurons in the inferior temporal cortex in short term and serial recognition memory tasks. *Exp Brain Res* 65: 614–622, 1987.
- Bruce CJ, Goldberg ME. Primate frontal eye fields. I. Single neurons discharging before saccades. *J Neurophysiol* 53: 603–635, 1985.
- Bruce CJ, Goldberg ME, Bushnell MC, Stanton GB. Primate frontal eye fields. II. Physiological and anatomical correlates of electrically evoked eye movements. *Brain Res* 54: 714–734, 1985.
- Brown MW, Wilson FAW, Riches IP. Neuronal evidence that inferomedial temporal cortex is more important than hippocampus in certain processes underlying recognition memory. *Brain Res* 409: 158–162, 1987.
- Bushnell MC, Goldberg ME, Robinson DL. Behavioral enhancement of visual responses in monkey cerebral cortex. I. Modulation in posterior parietal cortex related to selective visual attention. *J Neurophysiol* 46: 755–772, 1981.
- Carrasco M, McElree B. Covert attention accelerates the rate of visual information processing. *Proc Natl Acad Sci USA* 98: 5363–5367, 2001.
- Coenen AM, Eijkman EG. Cat optic tract and geniculate unit responses corresponding to human visual masking effects. *Exp Brain Res* 15: 441–451, 1972.
- Crist CF, Yamasaki DS, Komatsu H, Wurtz RH. A grid system and a microsyringe for single cell recording. *J Neurosci Methods* 26: 117–122, 1988.
- Cynader M, Berman N. Receptive-field organization of monkey superior colliculus. *J Neurophysiol* 35: 187–201, 1972.
- Diamond MR, Ross J, Morrone MC. Extraretinal control of saccadic suppression. *J Neurosci* 20: 3449–3455, 2000.
- Dorris MC, Klein RM, Everling S, Munoz DP. Contribution of the primate superior colliculus to inhibition of return. *J Cogn Neurosci* 14: 1256–1263, 2002.
- Fecteau JH, Bell AH, Munoz DP. Neural correlates of the automatic and goal-driven biases in orienting spatial attention. *J Neurophysiol* 92: 1728–1737, 2004.
- Fecteau JH, Munoz DP. Correlates of capture of attention and inhibition of return across stages of visual processing. *J Cogn Neurosci* 17: 1714–1727, 2005.
- Fehmi LG, Adkins JW, Lindsley DB. Electrophysiological correlates of visual perceptual masking in monkeys. *Exp Brain Res* 7: 299–316, 1969.
- Fortune ES, Rose GJ. Short-term synaptic plasticity as a temporal filter. *Trends Neurosci* 24: 381–385, 2001.
- Georg K, Lappe M. Spatio-temporal contingency of saccade-induced chronotaxis. *Exp Brain Res* 180: 535–539, 2007.
- Glantz SA. *Primer of Biostatistics*. New York: McGraw-Hill, 2002, p. xviii.
- Hartline HK, Wagner HG, Ratliff F. Inhibition in the eye of limulus. *J Gen Physiol* 39: 651–673, 1956.
- Hays AV, Richmond BJ, Optican L. A UNIX-based multiple process system for real-time data acquisition and control. *WESCON Conf Proc* 2: 1–10, 1982.
- Hikosaka O, Wurtz RH. Visual and oculomotor functions of monkey substantia nigra pars reticulata. I. Relation of visual and auditory responses to saccades. *J Neurophysiol* 49: 1230–1253, 1983.
- Ivry RB, Spencer RM. The neural representation of time. *Curr Opin Neurobiol* 14: 225–232, 2004.
- Jahanshahi M, Jones CRG, Dirnberger G, Frith CD. The substantia nigra pars compacta and temporal processing. *J Neurosci* 26: 12266–12273, 2006.
- Judge SJ, Richmond BJ, Chu FC. Implantation of magnetic search coils for measurement of eye position: an improved method. *Vision Res* 20: 535–538, 1980b.
- Judge SJ, Wurtz RH, Richmond BJ. Vision during saccadic eye movements. I. Visual interactions in striate cortex. *J Neurophysiol* 43: 1133–1155, 1980a.
- Klein RM. Inhibition of return. *Trends Cogn Sci* 4: 138–147, 2000.
- Kohn A. Visual adaptation: physiology, mechanism, and functional benefits. *J Neurophysiol* 97: 3155–3164, 2007.
- Li L, Miller EK, Desimone R. The representation of stimulus familiarity in anterior inferior temporal cortex. *J Neurophysiol* 69: 1918–1929, 1993.
- LSR. Information on LSR custom microdrive system. Available at ftp://lsr-ftp.nei.nih.gov/lsr/StepperDrive/. Accessed April 18, 2008.
- Lynch JC, Hoover JE, Strick PL. Input to the primate frontal eye field from the substantia nigra, superior colliculus, and dentate nucleus demonstrated by transneuronal transport. *Exp Brain Res* 100: 181–186, 1994.
- MacPherson JM, Aldridge JW. A quantitative method of computer analysis of spike train data collected from behaving animals. *Brain Res* 175: 183–187, 1979.
- Marlin SG, Douglas RM, Cynader MS. Position-specific adaptation in simple cell receptive fields of the cat striate cortex. *J Neurophysiol* 66: 1769–1784, 1991.
- Matell MS, Meck WH. Cortico-striatal circuits and interval timing: coincidence detection of oscillatory processes. *Brain Res Cogn Brain Res* 21: 139–170, 2004.
- Matin E, Clymer AB, Matin L. Metacontrast and saccadic suppression. *Science* 178: 179–182, 1972.
- Mayo JP. Two's a crowd: suppressed V4 visual responses to sequential stimuli. *J Neurosci* 27: 723–724, 2007.
- Mays LE, Sparks DL. Dissociation of visual and saccade-related responses in superior colliculus neurons. *J Neurophysiol* 43: 207–232, 1980.
- Mohler CW, Goldberg ME, Wurtz RH. Visual receptive fields of frontal eye field neurons. *Brain Res* 61: 385–389, 1973.
- Morrone MC, Ross J, Burr D. Saccadic eye movements cause compression of time as well as space. *Nat Neurosci* 8: 950, 2005.
- Motter BC. Modulation of transient and sustained response components of V4 neurons by temporal crowding in flashed stimulus sequences. *J Neurosci* 26: 9683–9694, 2006.
- Movshon JA, Lennie P. Pattern-selective adaptation in visual cortical neurons. *Nature* 278: 850–852, 1979.
- Muller JR, Metha AB, Krauskopf J, Lennie P. Rapid adaptation in visual cortex to the structure of images. *Science* 285: 1405–1408, 1999.
- Priebe NJ, Churchland MM, Lisberger SG. Constraints on the source of short-term motion adaptation in macaque area MT. I. The role of input and intrinsic mechanisms. *J Neurophysiol* 88: 354–369, 2002.
- Ratliff F. Contour and contrast. *Sci Am* 226: 91–101, 1972.
- Richmond BJ, Wurtz RH. Vision during saccadic eye movements. II. A corollary discharge to monkey superior colliculus. *J Neurophysiol* 43: 1156–1167, 1980.
- Ringo JL. Stimulus specific adaptation in inferior temporal and medial temporal cortex of the monkey. *Behav Brain Res* 76: 191–197, 1996.
- Robinson DA. Eye movements evoked by collicular stimulation in the alert monkey. *Vision Res* 12: 1795–1808, 1972.
- Robinson DL, Kertzman C. Covert orienting of attention in macaques. III. Contributions of the superior colliculus. *J Neurophysiol* 74: 713–721, 1995.
- Sakamoto Y, Ishiguro M, Kitagawa G. *Akaike Information Criterion Statistics*. Boston, MA: KTK Scientific Publishers, 1986, p. xix.
- Schall JD. The neural selection and control of saccades by the frontal eye field. *Philos Trans R Soc Lond B Biol Sci* 357: 1073–1082, 2002.
- Schall JD, Morel A, King DJ, Bullier J. Topography of visual cortex connections with frontal eye field in macaque: convergence and segregation of processing streams. *J Neurosci* 15: 4464–4487, 1995.
- Schiller PH. Single unit analysis of backward visual masking and metacontrast in the cat lateral geniculate nucleus. *Vision Res* 8: 855–866, 1968.
- Sommer MA, Wurtz RH. Composition and topographic organization of signals sent from the frontal eye field to the superior colliculus. *J Neurophysiol* 83: 1979–2001, 2000.
- Sommer MA, Wurtz RH. A pathway in primate brain for internal monitoring of movements. *Science* 296: 1480–1482, 2002.

- Sommer MA, Wurtz RH.** What the brain stem tells the frontal cortex. I. Oculomotor signals sent from superior colliculus to frontal eye field via mediodorsal thalamus. *J Neurophysiol* 91: 1381–1402, 2004.
- Sommer MA, Wurtz RH.** Influence of the thalamus on spatial visual processing in frontal cortex. *Nature* 444: 374–377, 2006.
- Spitzer H, Desimone R, Moran J.** Increased attention enhances both behavioral and neuronal performance. *Science* 240: 338–340, 1988.
- Stanton GB, Goldberg ME, Bruce CJ.** Frontal eye field efferents in the macaque monkey. I. Subcortical pathways and topography of striatal and thalamic terminal fields. *J Comp Neurol* 271: 473–492, 1988.
- Stelmach LB, Herdman CM.** Directed attention and perception of temporal order. *J Exp Psychol* 17: 539–550, 1991.
- Thompson KG, Schall JD.** The detection of visual signals by macaque frontal eye field during masking. *Nat Neurosci* 2: 283–288, 1999.
- Titchener EB.** *Lectures on the Elementary Psychology of Feeling and Attention*. New York: MacMillan, 1908, p. ix.
- Umeno MM, Goldberg ME.** Spatial processing in the monkey frontal eye field. I. Predictive visual responses. *J Neurophysiol* 78: 1373–1383, 1997.
- Umeno MM, Goldberg ME.** Spatial processing in the monkey frontal eye field. II. Memory responses. *J Neurophysiol* 86: 2344–2352, 2001.
- Ungerleider LG, Galkin TW, Desimone R, Gattass R.** Cortical connections of area V4 in the macaque. *Cereb Cortex* 18: 477–499, 2008.
- Wark B, Lundstrom BN, Fairhall A.** Sensory adaptation. *Curr Opin Neurobiol* 17: 423–429, 2007.
- Wiggs CL, Martin A.** Properties and mechanisms of perceptual priming. *Curr Opin Neurobiol* 8: 227–233, 1998.
- Wurtz RH, Richmond BJ, Judge SJ.** Vision during saccadic eye movements. III. Visual interactions in monkey superior colliculus. *J Neurophysiol* 43: 1168–1181, 1980.
- Xiang JZ, Brown MW.** Differential neuronal encoding of novelty, familiarity and recency in regions of the anterior temporal lobe. *Neuropharmacology* 37: 657–676, 1998.
- Xiao Q, Barborica A, Ferrera VP.** Radial motion bias in macaque frontal eye field. *Vis Neurosci* 23: 49–60, 2006.
- Yarrow K, Haggard P, Heal R, Brown P, Rothwell JC.** Illusory perceptions of space and time preserve cross-saccadic perceptual continuity. *Nature* 414: 302–305, 2001.
- Yarrow K, Johnson H, Haggard P, Rothwell JC.** Consistent chronostasis effects across saccade categories imply a subcortical efferent trigger. *J Cogn Neurosci* 16: 839–847, 2004.
- Zucker RS.** Short-term synaptic plasticity. *Annu Rev Neurosci* 12: 13–31, 1989.